# Comparison of triton bound state properties using different separable representations of realistic potentials

#### W. Schadow

Institute of Nuclear and Particle Physics, and Department of Physics, Ohio University, Athens, OH 45701

#### W. Sandhas

Physikalisches Institut der Universität Bonn, Endenicher Allee 11-13, D-53115 Bonn, Germany

### J. Haidenbauer

Institut für Kernphysik, Forschungszentrum Jülich GmbH, D-52425 Jülich, Germany

# A. Nogga

Institut für Theoretische Physik II, Ruhr-Universität Bochum, D-44780 Bochum, Germany (October 22, 1998)

# Abstract

The quality of two different separable expansion methods (W matrix and Ernst-Shakin-Thaler) is investigated. We compare the triton binding energies and components of the triton wave functions obtained in this way with the results of a direct two-dimensional treatment. The Paris, Bonn A and Bonn B potentials are employed as underlying two-body interactions, their total angular momenta being incorporated up to  $j \leq 2$ . It is found that the most accurate results based on the Ernst-Shakin-Thaler method agree within 1.5% or better with the two-dimensional calculations, whereas the results for the W-matrix representation are less accurate.

PACS number(s): 21.60.-n, 27.10.+h

#### I. INTRODUCTION

Separable approximations or expansions of the underlying two-body interaction play an essential role in calculations of few-nucleon systems. In the three-body problem such an input reduces the two-dimensional Faddeev equations, or the corresponding Alt-Grassberger-Sandhas (AGS) equations, to one-dimensional effective two-body equations [1]. Analogously, the four-body AGS equations go over into effective three-body, and, after repeated application of separable expansions, into effective two-body equations [2]. A considerable reduction of the complexity of the original problem is achieved in this way. What remains to be done, however, is a careful test of accuracy of the respective separable representations.

In early calculations Yamaguchi-type separable potentials were employed. Though not very realistic, they simulated characteristic aspects of the nuclear interaction, leading thus to qualitatively correct cross sections for three-nucleon scattering. Stimulated by this experience, rather sophisticated separable approximation or expansion techniques were developed and have been applied successfully to realistic interactions.

The Ernst-Shakin-Thaler (EST) expansion [3] is considered as a particularly powerful separable approach. Its efficiency has been thoroughly investigated for the Paris potential [4]. Indeed, based on high-rank separable expansions of this type [5,6], rather accurate predictions for the neutron-deuteron (n-d) cross section and some polarization observables were achieved [6,7]. Later on, when direct solutions of the two-dimensional three-body equations became available [8], it was established that the results obtained in this way and with the EST approach are in excellent agreement [9,10].

The W-matrix method [11] provides quite directly a rank-one separable representation of the two-body T matrix, which preserves the analytical properties of the original T matrix. For the Malfliet-Tjon (MT I+III) potential three-body bound-state and scattering results [12,13], including break-up [14], were obtained on this basis in complete agreement with alternative treatments. Calculations for the Paris potential were also found to be rather reliable for most, but not all observables [13].

For further applications of separable approximations or expansions, e.g., in processes as the photodisintegration of three-nucleon systems [15,16], the corresponding radiative capture [17], or the pion absorption on such systems [18], additional tests of accuracy of the three-body wave functions involved appear desirable. In case of a 5 channel calculation and the EST method such a test has been made already in Ref. [19] for the Paris potential, and, with a modified expansion method, in Ref. [20] for the Argonne 14 potential restricted to  $j \leq 2$ .

In what follows we compare triton bound-state calculations performed by means of the EST expansion and the W-matrix approximation with direct solutions of the twodimensional homogeneous three-body equations. In view of the sensitivity of the bound-state problem to differences in the two-body input, this comparison should provide a particularly relevant test of accuracy of these methods.

The paper is organized as follows: Sections II and III briefly describe the W-matrix and EST methods, respectively. In Sec. IV we give the relevant equations for the bound-state calculations using separable potentials (details of the direct treatment can be found in Refs. [21,22]). Our results and conclusions are presented in the last section.

#### II. W-MATRIX REPRESENTATION

The W-matrix method [11,13] leads to a quite appropriate splitting of the two-body T matrix into one dominant separable part and a small non-separable remainder

$$T_{ll'}(p, p'; E + i0) = {}^{S}T_{ll'}(p, p'; E + i0) + {}^{R}T_{ll'}(p, p'; E + i0).$$
(2.1)

Similarly to the T matrix, the W matrix is defined by an equation of Lippmann-Schwinger type, however, with a modified non-singular kernel. After partial wave decomposition this equation is given by (we use units  $(\hbar c)^2 = 2\mu = 1$  and thus  $E = p^2$ )

$$W_{l\hat{l}}^{\eta}(p,p';E) = U_{l\hat{l}}^{\eta}(p,p') + \sum_{l'} \int_{0}^{\infty} dq \, q^{2} \, \frac{U_{ll'}^{\eta}(p,q) - U_{ll'}^{\eta}(p,k)}{E - q^{2}} \, q^{2l'} \, W_{l'\hat{l}}^{\eta}(q,p';E), \tag{2.2}$$

where k is subject to the constraint  $k = \sqrt{E}$  for  $E \ge 0$  and is kept arbitrary for E < 0. Here l and  $\hat{l}$  are the orbital angular momenta, and  $\eta = (s, j; t)$  stands for the spin, the angular momentum j [ with the coupling sequence (l, s)j], and the isospin t of the two-body subsystem. The input entering Eq. (2.2) is related to the two-body potential matrix  $V_{l\hat{l}}^{\eta}(p, p')$  according to  $U_{l\hat{l}}^{\eta}(p, p') = p^{-l}V_{l\hat{l}}^{\eta}(p, p')p'\hat{l}$ . The separable part of the W-matrix representation (2.1) of the two-body T matrix is given by

$${}^{S}T^{\eta}_{ll'}(p,p';E+i0) = \sum_{\hat{ll'}} p^{l} W^{\eta}_{l\hat{l}}(p,k;E) \Delta^{\eta}_{\hat{l}\hat{l}'}(E+i0) W^{\eta}_{l'\hat{l}'}(p',k;E) p'^{l'}$$
(2.3)

and the nonseparable remainder reads

$${}^{\mathrm{R}}T^{\eta}_{ll'}(p,p';E+i0) = p^{l} \left[ W^{\eta}_{ll'}(p,p';E) - \sum_{\hat{l}\hat{l}'} W^{\eta}_{l\hat{l}}(p,k;E) \left( W^{\eta}_{\hat{l}\hat{l}'}(k,k;E) \right)^{-1} W^{\eta}_{\hat{l}'l'}(p',k;E) \right] p'^{l'}.$$
(2.4)

The propagator  $\Delta_{\hat{l}\hat{l}'}^{\eta}$  is given by

$$\Delta_{\hat{l}\hat{l}'}^{\eta} = \sum_{\hat{l}''} (F_{\hat{l}\hat{l}''}^{\eta}(E+i0))^{-1} (W_{\hat{l}\hat{l}''}^{\eta}(k,k;E))^{-1}, \tag{2.5}$$

where  $F^{\eta}_{\hat{l}\hat{l}''}(E+i0)$  is a generalization of the Jost function

$$(F_{\hat{l}\hat{l}'}^{\eta}(E+i0))^{-1} = \delta_{\hat{l}\hat{l}'} - \int_{0}^{\infty} dq \, q^2 \, q^{2\hat{l}} \, \frac{W_{\hat{l}\hat{l}'}(q,k;E)}{E+i0-q^2} \,. \tag{2.6}$$

On-the-energy-shell and half-off-shell the separable part (2.3) of (2.1) is identical with the exact T matrix. In fact, when inserting the momentum  $k = \sqrt{E}$  for one or both of the momenta p or p', we easily see that the remainder (2.4) vanishes. Therefore, the separable part of the T matrix has the same pole and cut structure as the full T matrix. This suggests to approximate the T matrices, entering the kernel of Faddeev-type equations, by the separable expression (2.3). To optimize this approximation, i.e., to minimize the effect of the neglected remainder, two criteria for the choice of the functional form of the free parameter k were developed [13]. In the present work we apply the criterion based on the Schmidt norm of the kernel of the three-body equations.

In the past this method has been used in elastic n-d scattering calculations [12,13], in the breakup case [14], and more recently in the photodisintegration of the triton [15].

#### III. EST METHOD

The Ernst-Shakin-Thaler (EST) method [3] allows one to generate separable representations of arbitrary rank N that agree exactly (on- and half-off-shell) with the original T matrix at N specific, appropriately chosen energies.

For a brief outline of this method let us begin with the (partial-wave projected) Lippmann-Schwinger equation for the wave function,

$$|\psi_E\rangle = |k_E\rangle + G_0(E)V|\psi_E\rangle,\tag{3.1}$$

where  $|k_E\rangle$  is the incoming wave, and  $G_0(E)$  the two-body Green's function. The dependence on the orbital angular momenta l, l' and on the conserved quantum numbers (the spin, the angular momentum j [ with the coupling sequence (l,s)j], and the isospin t of the two-body subsystem) is suppressed for convenience. For proper scattering solutions (on-shell),  $k_E$  and E are related by  $E = k_E^2$ .

According to the EST method, a rank-N separable representation of a potential V is given by the form

$$V^{\text{EST}} = \sum_{\mu,\nu=1}^{N} V |\psi_{E_{\mu}}\rangle \Lambda_{\mu\nu} \langle \psi_{E_{\nu}} | V, \qquad (3.2)$$

where  $E_{\mu}$ ,  $(\mu = 1, ..., N)$ , is a freely choosable, but fixed set of energies. The coupling strengths  $\Lambda_{\mu\nu}$  are determined by the condition

$$\sum_{\nu=1}^{N} \Lambda_{\mu\nu} \langle \psi_{E_{\nu}} | V | \psi_{E_{\rho}} \rangle = \delta_{\mu\rho}. \tag{3.3}$$

Note that the "form factors" in the separable potential (3.2) consist of the objects  $V|\psi_{E_{\mu}}\rangle$ , where  $|\psi_{E_{\mu}}\rangle$  are solutions of Eq. (3.1) at the energies  $E=E_{\mu}$ . Thus, Eq. (3.3) together with Eq. (3.2) implies that the following relation holds at the N energies  $E_{\mu}$ 

$$V^{\text{EST}}|\psi_{E_{\mu}}\rangle = V|\psi_{E_{\mu}}\rangle = T(E_{\mu})|k_{E_{\mu}}\rangle = T^{\text{EST}}(E_{\mu})|k_{E_{\mu}}\rangle. \tag{3.4}$$

Here T and  $T^{\text{EST}}$  are the two-body T matrices for the potential V and its separable representation  $V^{\text{EST}}$ , respectively. Evidently Eq. (3.4) means that the on-shell, as well as the

half-off-shell T matrices for both interactions, V and  $V^{\text{EST}}$ , are exactly the same at the energies  $E_{\mu}$ .

With the form factors  $|g_{\nu}^{\eta}l\rangle = V^{\eta}|\psi_{E_{\nu}}^{\eta}\rangle_{l}$   $(\eta = (s, j; t))$  and the propagators  $\Delta_{\mu\nu}^{\eta}$  of this representation, the two-body T matrix reads

$$T_{ll'}^{\eta}(E+i0) = \sum_{\mu\nu} |g_{\mu}^{\eta}l\rangle \,\Delta_{\mu\nu}^{\eta}(E+i0) \,\langle g_{\nu}^{\eta}l'| \qquad (3.5)$$

where

$$\boldsymbol{\Delta}^{\eta}(E+i0) = \left( (\boldsymbol{\Lambda}^{\eta})^{-1} - \mathcal{G}_{\mathbf{0}}(E+i0) \right)^{-1}$$
(3.6)

and

$$(\mathcal{G}_0(E+i0))_{\mu\nu} = \sum_{l} \langle g_{\mu} l | G_0(E+i0) | g_{\nu} l \rangle).$$
 (3.7)

For more details of this construction we refer to Refs. [4,5]. The chosen approximation energies  $E_{\mu}$  for the interaction models considered in the present study are summarized in Table I. These energies completely specify the separable expansion (3.2) Note that, for reasons of convenience, we have represented the (numerically given) form factors analytically (cf. Eqs. (2.1) and (2.2) of Ref. [6]), and have performed the actual calculations with these expressions. The corresponding parametrizations can be obtained from one of the authors (J.H.) on request.

In Sec. V we are going to present three-nucleon bound state results, based on the EST representation, with a varying rank in various two-body partial waves. We characterize these representations by  $(n_1n_2n_3...)$ , where  $n_1$ ,  $n_2$ ,  $n_3$ , ... stand for the ranks in the  ${}^1s_0$ ,  ${}^3s_1 - {}^3d_1$ ,  ${}^1p_1$ ,  ${}^3p_0$ ,  ${}^3p_1$ ,  ${}^1d_2$ ,  ${}^3d_2$ , and  ${}^3p_2 - {}^3f_2$  NN partial waves. For a specific rank  $n_\mu$  in a certain partial wave the approximation energies  $E_\mu$  can be read off from Table I. They are given by the first  $n_\mu$  entries. The notation in the results of the three-body calculations is done in the same order of the partial waves, but the ranks of the unused partial waves are left out.

#### IV. 3N BOUND-STATE CALCULATION

The triton bound state  $|\Psi_t\rangle$  is determined by the eigenvalue equation

$$(E_{t} - H) |\Psi_{t}\rangle = 0, \tag{4.1}$$

where the total Hamiltonian H is given by  $H = H_0 + V = H_0 + \sum_{\gamma=1}^{3} V_{\gamma}$ . Here we have used the complementary notation  $V_{\gamma} = V_{\alpha\beta}$  for the two-body potentials, while  $H_0$  denotes the free three-body Hamiltonian. When introducing the corresponding resolvent  $G_0(z) = (z - H_0)^{-1}$  or the channel resolvents  $G_{\gamma}(z) = (z - H_0 - V_{\gamma})^{-1}$ , Eq. (4.1) can be written in form of homogeneous integral equations,

$$|\Psi_{\rm t}\rangle = G_0(E_{\rm t}) V |\Psi_{\rm t}\rangle = G_0(E_{\rm t}) \sum_{\gamma} V_{\gamma} |\Psi_{\rm t}\rangle$$
 (4.2)

$$|\Psi_{\rm t}\rangle = G_{\gamma}(E_{\rm t})\,\bar{V}_{\gamma}\,|\Psi_{\rm t}\rangle = G_{\gamma}(E_{\rm t})\sum_{\beta} (1 - \delta_{\gamma\beta})\,V_{\beta}\,|\Psi_{\rm t}\rangle,$$
 (4.3)

with  $\bar{V}_{\gamma} = V - V_{\gamma}$  being the channel interaction between particle  $\gamma$  and the  $(\alpha\beta)$  subsystem. The latter equation can also be understood as a representation of the bound state by the "form-factors"  $|F_{\gamma}\rangle = \bar{V}_{\gamma} |\Psi_{\rm t}\rangle$ ,

$$|\Psi_{\rm t}\rangle = G_{\gamma}(E_{\rm t})|F_{\gamma}\rangle.$$
 (4.4)

Multiplying this representation with  $(1 - \delta_{\beta\gamma})V_{\gamma}$ , using the relation  $V_{\gamma}G_{\gamma} = T_{\gamma}G_{0}$ , and summing over  $\gamma$ , we obtain for  $|F_{\beta}\rangle$  the coupled set of homogeneous integral equations

$$|F_{\beta}\rangle = \sum_{\gamma} (1 - \delta_{\beta\gamma}) T_{\gamma}(E_{t}) G_{0}(E_{t}) |F_{\gamma}\rangle. \tag{4.5}$$

Note that this relation may alternatively be derived by going to the bound-state poles of the AGS equations, providing thus their homogeneous version [1]. From (4.2) and (4.4) we infer that the solutions of Eq. (4.5) provide  $|\Psi_t\rangle$  according to

$$|\Psi_{\rm t}\rangle = \sum_{\gamma} G_0(E_{\rm t}) T_{\gamma}(E_{\rm t}) G_0(E_{\rm t}) |F_{\gamma}\rangle = \sum_{\gamma} |\psi_{\gamma}\rangle. \tag{4.6}$$

The  $|\psi_{\gamma}\rangle$  are the standard Faddeev components, as seen by using the definition of  $|F_{\gamma}\rangle$  and the relation (4.3),

$$|\psi_{\gamma}\rangle = G_0 T_{\gamma} G_0 |F_{\gamma}\rangle = G_0 V_{\gamma} G_{\gamma} |F_{\gamma}\rangle = G_0 V_{\gamma} G_{\gamma} \bar{V}_{\gamma} |\Psi_{t}\rangle = G_0 V_{\gamma} |\Psi_{t}\rangle. \tag{4.7}$$

Equation (4.5) will be treated numerically in momentum space, employing a complete set of partial-waves states  $|p q l b \Gamma I\rangle$ . The label b denotes the set  $(\eta KL)$  of quantum numbers, where K and L are the channel spin of the three nucleons [with the coupling sequence  $(j, \frac{1}{2})K$ ] and the relative angular momentum between the two-body subsystem and the third particle, respectively.  $\Gamma$  is the total angular momentum following from the coupling sequence  $(K, L)\Gamma$ , and I is the total isospin. These states satisfy the completeness relation

$$1 = \sum_{bl\Gamma I} \int_{0}^{\infty} \int_{0}^{\infty} dp \, p^2 \, dq \, q^2 \, |p \, q \, l \, b \, \Gamma \, I\rangle \langle p \, q \, l \, b \, \Gamma \, I|. \tag{4.8}$$

The required antisymmetry under permutation of two particles in the subsystem can be achieved by choosing only those states which satisfy the condition  $(-)^{l+s+t} = -1$ . Table II contains the quantum numbers of the corresponding channels taken into account.

Inserting the separable T matrix (3.5) for the EST potentials and defining

$$F_{\beta}^{\mu b}(q) = \sum_{l} \int_{0}^{\infty} dp \, p^2 \, g_{l\mu}^{\eta}(p) \, \langle p \, q \, l \, b \, \Gamma I | G_0 | F_{\beta} \rangle, \tag{4.9}$$

Eq. (4.5) goes over into

$$F^{\mu b}(q) = \sum_{b'} \sum_{\nu \rho} \int_{0}^{\infty} dq' \, q'^2 \, \mathcal{A} \mathcal{V}_{\mu \nu}^{bb'}(q, q', E_{\rm t}) \, \Delta_{\nu \rho}^{\eta'}(E_{\rm t} - \frac{3}{4}q'^2) \, F^{\rho b'}(q'), \tag{4.10}$$

with

$$\mathcal{AV}_{\mu\nu}^{bb'}(q,q',E_{t}) = 2\sum_{ll'} \int_{0}^{\infty} \int_{0}^{\infty} dp \, p^{2} \, dp' \, p'^{2} \, g_{l\mu}^{\eta}(p) \, \langle p \, q \, l \, b \, \Gamma \, I | G_{0}(E_{t}) | p' \, q' \, l' \, b' \, \Gamma \, I \rangle \, g_{l'\nu}^{\eta'}(p') \quad (4.11)$$

being the so-called effective potential. The recoupling coefficients entering this equation can be found in Ref. [13] (or in a more compact form in [21] for another coupling sequence which can easily be changed to the present one). In case of the W-matrix representation Eqs. (4.10) and (4.11) are of similar form and, therefore, not given here.

After discretization Eq. (4.10) can be treated as a linear eigenvalue problem, where the energy is considered as a parameter which is varied until the corresponding eigenvalue equals unity. The eigenvalues can be found by using standard numerical algorithms. A better approach is an iterative treatment, known as "power method" [23], which is justified due to the compactness of the kernel of the integral equation employed. It was found that this method is much faster than standard eigenvalue algorithms and yields the same accuracy. For the direct solution of the two-dimensional Faddeev equations we used a Lanczos-type algorithm [24,25] that is even more efficient.

For the integration in Eq. (4.10) a standard Gauss-Legendre mesh was chosen. The angular integration in the effective potential was done with 16 grid points. Table III contains results for the Paris (EST) potential for different numbers of partial wave and an increasing number of mesh points for the q integration. In all cases 36 grid points were sufficient to get the binding energy up to 5 significant figures. For all further calculations we have used 40 mesh points to get wave functions of high accuracy. In the calculations we also included q = 0 to avoid extrapolations for small momenta in further applications. The same was done for both variables in the calculation of the wave function. The binding energies obtained in EST and W-matrix approximation for different potentials are given in Tables IV-VI, compared with results from a two-dimensional treatment [21] of the Faddeev equations.

The whole wave function can now be calculated by either using Eq. (4.6), or by applying the permutation operator P on one Faddeev component [21]

$$|\Psi_{\rm t}\rangle = (1+P)|\psi_1\rangle,\tag{4.12}$$

where P represents the sum of all cyclical and anticyclical permutations of the nucleons. From the practical point of view the latter method has to be preferred. Once  $|\psi_1\rangle$  is computed from  $|\psi_1\rangle = G_0(E_{\rm t}) T_1(E_{\rm t}) G_0(E_{\rm t}) |F_1\rangle$  the calculation of the full wave wave function via Eq. (4.12) is independent of the rank of the separable approximation, which considerably reduces the computing time.

The wave function is normalized according to

$$\langle \Psi_{t} | \Psi_{t} \rangle = \sum_{\gamma} \langle \psi_{\gamma} | \Psi_{t} \rangle = 3 \langle \psi_{1} | \Psi_{t} \rangle = 1.$$
 (4.13)

It should be noted that, inserting the completeness relation (4.8) into  $\langle \Psi_t | \Psi_t \rangle$ , one has to deal with an infinite number of states due to the resulting recouplings. In contrast, when inserting the completeness relation in  $\langle \psi_1 | \Psi_t \rangle$ , one has to deal with a finite number of partial waves corresponding to the ones in  $\langle \psi_1 |$ . Plots of the wave functions for the Paris (EST) and Bonn A (EST) potentials are shown in Figures 1 - 6. The figures for the Bonn B (EST) potential are not distinguishable by eye from the ones for the Bonn A (EST) potential, and are therefore not shown.

#### A. Properties of the wave function

It is common to investigate the properties of the wave function in the LS-coupling scheme (for simplicity we skip the dependence on the isospins in the notation, since they are not recoupled)

$$|p q ((lL) \mathcal{L}(sS) \mathcal{S}) \Gamma M_{\Gamma} \rangle.$$
 (4.14)

In this scheme first the two orbital angular momenta and the two spins are coupled separately. The total orbital angular momentum is then coupled with the total spin to the total angular momentum of the three-body system. The total angular momentum of the triton is  $\Gamma = 1/2$ , the total spin  $\mathcal{S}$  of three particles can be  $\mathcal{S} = 1/2$  or  $\mathcal{S} = 3/2$ . The total orbital angular momentum is, therefore, restricted to  $\mathcal{L} = 0, 1, 2$ .

The transformation from the channel spin into the LS coupling scheme is given by

$$\langle ((lL)\mathcal{L}, (sS)\mathcal{S})\Gamma M_{\Gamma}|$$

$$= \sum_{jK} (-)^{l+s+L+S+\mathcal{L}+S+1} \hat{j} \hat{\mathcal{L}} \hat{\mathcal{S}} \hat{K} \begin{cases} l & \mathcal{S} & K \\ S & j & s \end{cases} \begin{cases} l & \mathcal{S} & K \\ \Gamma & L & \mathcal{L} \end{cases} \langle (((ls)jS)KL)\Gamma M_{\Gamma}|, \qquad (4.15)$$

with the abbreviation  $\hat{j} = \sqrt{2j+1}$  used only in this equation. It should be noted that for this transformation the wave function (4.12) has to be projected on all states that give a contribution due to Eq. (4.15). Otherwise the normalization constant of the wave function is changed. It is not sufficient to use only those channels used in the calculation of the

Faddeev component. Here again the recoupling of channels, as in the calculation of the normalization constant, plays a role.

In the LS coupling scheme the wave function can be classified according to the contributions of the states belonging to  $\mathcal{L} = 0, 1, 2$ .

$$1 = 3 \langle \psi_{1} | \Psi_{t} \rangle$$

$$= 3 \sum_{\mathcal{L}} \sum_{S} \sum_{lLsS} \int_{0}^{\infty} \int_{0}^{\infty} dp \, p^{2} \, dq \, q^{2} \, \langle \psi_{1} | p \, q \, ((lL)\mathcal{L}(sS)\mathcal{S})\Gamma \rangle \, \langle p \, q \, ((lL)\mathcal{L}(Ss)\mathcal{S})\Gamma | \Psi_{t} \rangle$$

$$= \sum_{f} P(\mathcal{L}) = P(S) + P(S') + P(P) + P(D). \tag{4.16}$$

The contributions to the normalization constant for a certain total angular momentum are denoted by  $P(\mathcal{L})$ . In case of  $\mathcal{L} = 0$  also the symmetric and mixed symmetric spatial contributions P(S) and P(S'), are extracted. The antisymmetric part P(S'') of the wave function is negligible and, therefore, has been omitted. The main contribution to the mixed symmetric part stems from the difference between the  $^{1}s_{0}$  and the  $^{3}s_{1}$  interaction.

#### V. RESULTS AND CONCLUSIONS

As a test of accuracy of the EST and W-matrix approaches we compare the triton binding energies and wave functions obtained in this way with the results of a two-dimensional treatment of the Faddeev equations. In Tables IV-VI our binding energies obtained for the Paris, Bonn A, and Bonn B potentials are given for different combinations of partial waves. For all three potentials considered here, the EST results converge with increasing rank and agree within 0.2% with the two-dimensional results. In case of the W matrix, the free parameter k was chosen differently in each partial wave according to the criterion employed in Ref. [13], which consists in providing a binding energy close to the results obtained with other methods. This optimization method is not fully satisfactory in the  $j \leq 2$  calculations, due to ambiguities in fixing k when including the  ${}^3p_2$ - ${}^3f_2$  partial wave. The agreement of the W-matrix calculations with the two-dimensional results is less good than in the EST case. There are differences between  $0 \leq 4\%$ .

Our five-channel, i.e.,  $j \leq 1^+$ , calculations for the Paris (EST) potential are also in perfect agreement with the results by Parke et al. [19]. We can, moreover, compare with the results by Friar et al. [26] generated in coordinate space, and find again good agreement. For  $j \leq 2$  and the Paris potential our results are exactly the same as those of Ref. [10]. The binding energies for Bonn A and  $j \leq 2$  differ only slightly from those by Fonseca and Lehman [27].

For the Paris (EST), Bonn A (EST), Bonn B (EST) potentials the components of the three-body wave function, defined in the previous section, differ from the two-dimensional results by 0-2.5%, 0-0.05%, and 0-3% respectively. It should be emphasized, however, that only P(P) shows the large deviation of 3% quoted, while all other components are in much better agreement.

The W-matrix results for the components of the wave function differ by 0-12%, 0-10%, and 0-10% in case of the Paris, Bonn A, and Bonn B potentials, respectively. Here the largest deviations are found both in the P(P) and in the P(S') components.

Another test is given by the norm squared of the differences of the triton wave functions obtained in the separable and the two-dimensional treatments,  $\Delta N = ||\Psi_{\text{sep}} - \Psi_{2d}||^2$ . For the EST potentials  $\Delta N$  is of the order  $10^{-6}$ , while for the W-matrix representation it is of the order  $10^{-5}$ . Also in this respect the EST method, hence, leads to better results.

Thus, we have demonstrated the high quality of the EST expansion method. For  $j \leq 1^+$  and the Paris (EST) interaction this has been done already in [19], and for the Argonne potential (with a modified expansion scheme) in [20]. Here we have extended these former investigations up to  $j \leq 2$ , using moreover two versions of the Bonn potential. The accuracy achieved within the W-matrix approach is less satisfactory, namely of the order 2-10%. But it should be recalled that this treatment is based on a rather simple rank-one approximation only.

### ACKNOWLEDGMENTS

The work of W. S. and W. Sch., and that of A. N. was supported by the Deutsche Forschungsgemeinschaft under Grant Nos. Sa 327/23-1 and GL-8727-1, respectively. Part of this work has been done under the auspices of the U. S. Department of Energy under contract No. DE-FG02-93ER40756 with Ohio University. The numerical calculations were partly performed on the Cray T3E of the Höchstleistungsrechenzentrum in Jülich, Germany.

# REFERENCES

- [1] E. O. Alt, P. Grassberger, and W. Sandhas, Nucl. Phys. **B2**, 167 (1967).
- [2] P. Grassberger and W. Sandhas, Nucl. Phys. **B2**, 181 (1967).
- [3] D. J. Ernst, C. M. Shakin, and R. M. Thaler, Phys. Rev. C 8, 46 (1973); Phys. Rev. C 9, 1780 (1974).
- [4] J. Haidenbauer and W. Plessas, Phys. Rev. C 30, 1822 (1984).
- [5] J. Haidenbauer and Y. Koike, Phys. Rev. C 34, 1187 (1986).
- [6] Y. Koike, J. Haidenbauer, and W. Plessas, Phys. Rev. C 35, 396 (1987).
- [7] Y. Koike and J. Haidenbauer, Nucl. Phys. A463, 365c (1987).
- [8] H. Witała, T. Cornelius, and W. Glöckle, Few-Body Systems 3, 123 (1988).
- [9] T. Cornelius, W. Glöckle, J. Haidenbauer, Y. Koike, W. Plessas, and W. Witała, Phys. Rev. C 41, 2538 (1990).
- [10] S. Nemoto, K. Chmielewski, N. W. Schellingerhout, J. Haidenbauer, S. Oryu, and P. U. Sauer, Few-Body Systems, in press (1998).
- [11] E. A. Bartnik, H. Haberzettl, and W. Sandhas, Phys. Rev. C 34, 1520 (1986).
- [12] E. A. Bartnik, H. Haberzettl, T. Januschke, U. Kerwath, and W. Sandhas, Phys. Rev. C 36, 1678 (1987).
- [13] Th. Januschke, T. N. Frank, W. Sandhas, and H. Haberzettl, Phys. Rev. C 47, 1401 (1993).
- [14] T. N. Frank, H. Haberzettl, Th. Januschke, U. Kerwath, and W. Sandhas, Phys. Rev. C 38, 1112 (1988).
- [15] W. Schadow and W. Sandhas, Phys. Rev. C 55, 1074 (1997).

- [16] W. Sandhas, W. Schadow, G. Ellerkmann, L. L. Howell, and S. A. Sofianos, Nucl. Phys. A631, 210c (1998); W. Schadow and W. Sandhas, Nucl. Phys. A631, 588c (1998).
- [17] W. Schadow and W. Sandhas, to appear in Phys. Rev. C.
- [18] L. Canton and W. Schadow, Phys. Rev. C 56, 1231 (1997); L. Canton, G. Cattapan,
   G. Pisent, W. Schadow, and J. P. Svenne, Phys. Rev. C 57, 1588 (1998).
- [19] W. C. Parke, Y. Koike, D. R. Lehman, and L. C. Maximon, Few-Body Systems 11, 89 (1991).
- [20] Y. Koike, W. C. Parke, L. C. Maximon, and D. R. Lehman, Few-Body Systems 23, 53 (1997).
- [21] W. Glöckle, *The Quantum Mechanical Few-Body Problem* (Springer-Verlag, Berlin-Heidelberg, 1983).
- [22] A. Nogga, D. Hüber, H. Kamada, and W. Glöckle, Phys. Lett. B 409, 19 (1997).
- [23] R. A. Malfliet and J. A. Tjon, Nucl. Phys. **A127**, 161 (1969).
- [24] A. Stadler, W. Glöckle, and P. U. Sauer, Phys. Rev. C 44, 2319 (1991).
- [25] W. Saake, Diploma thesis (unpublished), Bochum University, 1992.
- [26] J. L. Friar, B. F. Gibson, and G. L. Payne, Phys. Rev. C 37, 2869 (1988).
- [27] A. C. Fonseca and D. R. Lehman, in Proceedings of the 14th International IUPAP Conference on Few-Body Problems in Physics, Williamsburg, VA 1994, Ed. Franz Gross (AIP, New York, 1995).

TABLES

			Paris pot	ential			
partial wave				$(E_{\mu},l_{\mu})$			
$^{1}s_{0}$	0	100	500	-100	-200		
$^{3}s_{1}-^{3}d_{1}$	$\epsilon_d$	(100,0)	(125,2)	(425,2)	(-50,0)	(-50,2)	
$^{1}p_{1}, ^{3}p_{1}$	10	-50	150	300	-150		
$^{3}p_{0}$	10	-50	150	350	-150		
$^{3}p_{2}-^{3}f_{2}$	(10,1)	(40,3)	(75,1)	(75,3)	(175,1)	(175,3)	(300,1)
$^{1}d_{2}, ^{3}d_{2}$	10	-50	150	300	-150		
		Во	onn $A$ and $B$	potentials			
partial wave				$(E_{\mu},l_{\mu})$			
$^{1}s_{0}$	0	100	300	-100	-50		
$^{3}s_{1}-^{3}d_{1}$	$\epsilon_d$	(50,2)	(100,0)	(300,2)	(-50,0)	(-50,2)	
$^{1}p_{1}, ^{3}p_{0}, ^{3}p_{1}$	10	-50	150	300	-150		
$^{3}p_{2}-^{3}f_{2}$	(10,1)	(10,3)	(75,1)	(75,3)	(150,1)	(150,3)	(200,1)
$^{1}d_{2}, ^{3}d_{2}$	10	-50	150	300	-150		

TABLE I. Approximation energies  $E_{\mu}$  used in the EST representations of the Paris, Bonn A and Bonn B potentials.  $\epsilon_d$  refers to the deuteron binding energy.  $E_{\mu}$  are lab energies in MeV. In case of coupled partial waves, the boundary condition chosen for the angular momentum  $l_{\mu}$  of the initial state (cf. Ref. [4]) is also specified.

Channel	Subsystem	l	s	$j^{\pi}$	au	K	L
1	$^{1}s_{0}$	0	0	0+	1	1/2	0
2	$^3s_1$	0	1	1+	0	1/2	0
3	$^3s_1$	0	1	1+	0	3/2	2
4	$^3d_1$	2	1	1+	0	1/2	0
5	$^3d_1$	2	1	1+	0	3/2	2
6	$^{3}p_{0}$	1	1	0-	1	1/2	1
7	$^1p_1$	1	0	1-	0	1/2	1
8	$^1p_1$	1	0	1-	0	3/2	1
9	$^3p_1$	1	1	1-	1	1/2	1
10	$^3p_1$	1	1	1-	1	3/2	1
11	$^1d_2$	2	0	$2^+$	1	3/2	2
12	$^{1}d_{2}$	2	0	$2^+$	1	5/2	2
13	$^3d_2$	2	1	$2^+$	0	3/2	2
14	$^3d_2$	2	1	$2^+$	0	5/2	2
15	$^3p_2$	1	1	$2^{-}$	1	3/2	1
16	$^3p_2$	1	1	$2^{-}$	1	5/2	3
17	$^3f_2$	3	1	$2^{-}$	1	3/2	1
18	$^3f_2$	3	1	$2^{-}$	1	5/2	3

TABLE II. Quantum numbers of the three-body channels.

# Meshpoints	$j \le 1^+$	$j \le 1$	$j \leq 2$
6	-8.3318	-8.1383	-9.0551
12	-7.3571	-7.1376	-7.4330
24	-7.3150	-7.0913	-7.3688
36	-7.3156	-7.0919	-7.3688
40	-7.3156	-7.0919	-7.3688

TABLE III. Triton binding energies (in MeV) with the Paris (EST) potential (56555557). The notation (56...) specifies the employed separable representation as explained in Sec. III.

		$E_{\rm t}({ m MeV})$	P(S)	P(S')	P(P)	P(D)
$j \le 1^+$	Paris (EST) (11)	-7.451	90.63	1.636	0.042	7.692
	Paris (EST) (34)	-7.266	89.88	1.652	0.065	8.402
	Paris (EST) (56)	-7.316	89.90	1.634	0.064	8.401
	Paris ( $W$ -matrix)	-7.300	90.22	1.450	0.064	8.265
	Paris	-7.297	89.88	1.625	0.066	8.428
	Paris-r	-7.310	89.88	1.623	0.066	8.428
$j \le 2^+$	Paris (EST) (1111)	-7.464	90.62	1.636	0.042	7.704
	Paris (EST) (3444)	-7.375	89.87	1.618	0.066	8.447
	Paris (EST) (5644)	-7.424	89.89	1.601	0.066	8.444
	Paris (EST) (5655)	-7.426	89.89	1.600	0.066	8.446
	Paris (W-matrix)	-7.343	90.21	1.436	0.064	8.288
	Paris	-7.408	89.87	1.591	0.068	8.474
$j \leq 1$	Paris (EST) (11111)	-7.464	90.83	1.468	0.044	7.658
	Paris (EST) (34333)	-7.074	90.28	1.492	0.064	8.167
	Paris (EST) (56444)	-7.093	90.30	1.488	0.062	8.154
	Paris (EST) (56555)	-7.092	90.30	1.488	0.062	8.153
	Paris $(W-matrix)$	-7.150	90.51	1.301	0.066	8.123
	Paris	-7.103	90.28	1.468	0.063	8.193
$j \leq 2$	Paris (EST) (11111111)	-7.549	90.61	1.459	0.047	7.879
	Paris (EST) (56555557)	-7.369	90.14	1.420	0.063	8.379
	Paris (W-matrix)	-7.088	90.54	1.366	0.062	8.034
	Paris	-7.378	90.11	1.403	0.064	8.418

TABLE IV. Triton wave function components for the Paris potential. The notation (56...) etc. specifies the employed separable (EST) representation as explained in Sec. III. The result for Paris-r is taken from Ref. [26].

		$E_{\rm t}({ m MeV})$	P(S)	P(S')	P(P)	P(D)
$j \le 1^+$	Bonn $A$ (EST) (11)	-8.350	92.75	1.415	0.028	5.811
	Bonn $A$ (EST) (44)	-8.347	92.35	1.427	0.034	6.188
	Bonn $A$ (EST) (56)	-8.380	92.31	1.432	0.035	6.220
	Bonn $A$ ( $W$ -matrix)	-8.371	92.01	1.385	0.041	6.565
	Bonn A	-8.378	92.32	1.426	0.035	6.217
$j \le 2^+$	Bonn A (EST) (1111)	-8.360	92.74	1.415	0.027	5.820
	Bonn $A$ (EST) (4444)	-8.411	92.35	1.411	0.034	6.204
	Bonn $A$ (EST) (5644)	-8.444	92.31	1.415	0.034	6.236
	Bonn A (W-matrix)	-8.399	92.00	1.380	0.039	6.578
	Bonn A	-8.443	92.32	1.411	0.035	6.235
$j \le 1$	Bonn A (EST) (11111)	-8.298	92.95	1.248	0.030	5.772
	Bonn $A$ (EST) (44444)	-8.083	92.72	1.252	0.037	5.995
	Bonn $A$ (EST) (56444)	-8.115	92.68	1.254	0.037	6.027
	Bonn A (W-matrix)	-8.160	92.36	1.209	0.043	6.391
	Bonn A	-8.127	92.69	1.248	0.037	6.029
$\overline{j \leq 2}$	Bonn A (EST) (11111111)	-8.395	92.81	1.264	0.031	5.895
	Bonn $A$ (EST) (56444445)	-8.285	92.59	1.236	0.037	6.135
	Bonn $A$	-8.295	92.59	1.231	0.037	6.138

TABLE V. Triton wave function components for the Bonn A potential. (56...) etc. specifies the employed separable (EST) representation as explained in Sec. III.

		$E_{\rm t}({ m MeV})$	P(S)	P(S')	P(P)	P(D)
$j \le 1^+$	Bonn $B$ (EST) (11)	-8.209	91.95	1.361	0.035	6.659
	Bonn $B$ (EST) (44)	-8.137	91.36	1.369	0.047	7.224
	Bonn $B$ (EST) (56)	-8.170	91.34	1.373	0.048	7.236
	Bonn $B$ ( $W$ -matrix)	-8.161	91.21	1.286	0.053	7.448
	Bonn $B$	-8.165	91.35	1.368	0.049	7.235
$j \le 2^+$	Bonn <i>B</i> (EST) (1111)	-8.219	91.94	1.360	0.034	6.668
	Bonn $B$ (EST) (4444)	-8.197	91.35	1.354	0.047	7.245
	Bonn $B$ (EST) (5644)	-8.230	91.34	1.357	0.048	7.256
	Bonn B (W-matrix)	-8.190	91.21	1.286	0.053	7.448
	Bonn B	-8.226	91.34	1.354	0.049	7.257
$j \le 1$	Bonn <i>B</i> (EST) (11111)	-8.159	92.14	1.200	0.037	6.620
	Bonn $B$ (EST) (44444)	-7.855	91.75	1.216	0.048	6.985
	Bonn $B$ (EST) (56444)	-7.884	91.74	1.218	0.048	6.700
	Bonn B (W-matrix)	-7.926	91.56	1.143	0.054	7.247
	Bonn B	-7.899	91.74	1.210	0.049	7.001
$j \leq 2$	Bonn B (EST) (11111111)	-8.282	91.96	1.208	0.039	6.791
	Bonn $B$ (EST) (56444445)	-8.088	91.61	1.189	0.048	7.149
	Bonn $B$ ( $W$ -matrix)	-7.919	91.56	1.143	0.052	7.249
	Bonn B	-8.103	91.62	1.184	0.048	7.152

TABLE VI. Triton wave function components for the Bonn B potential. (56...) etc. specifies the employed separable (EST) representation as explained in Sec. III.

# FIGURES

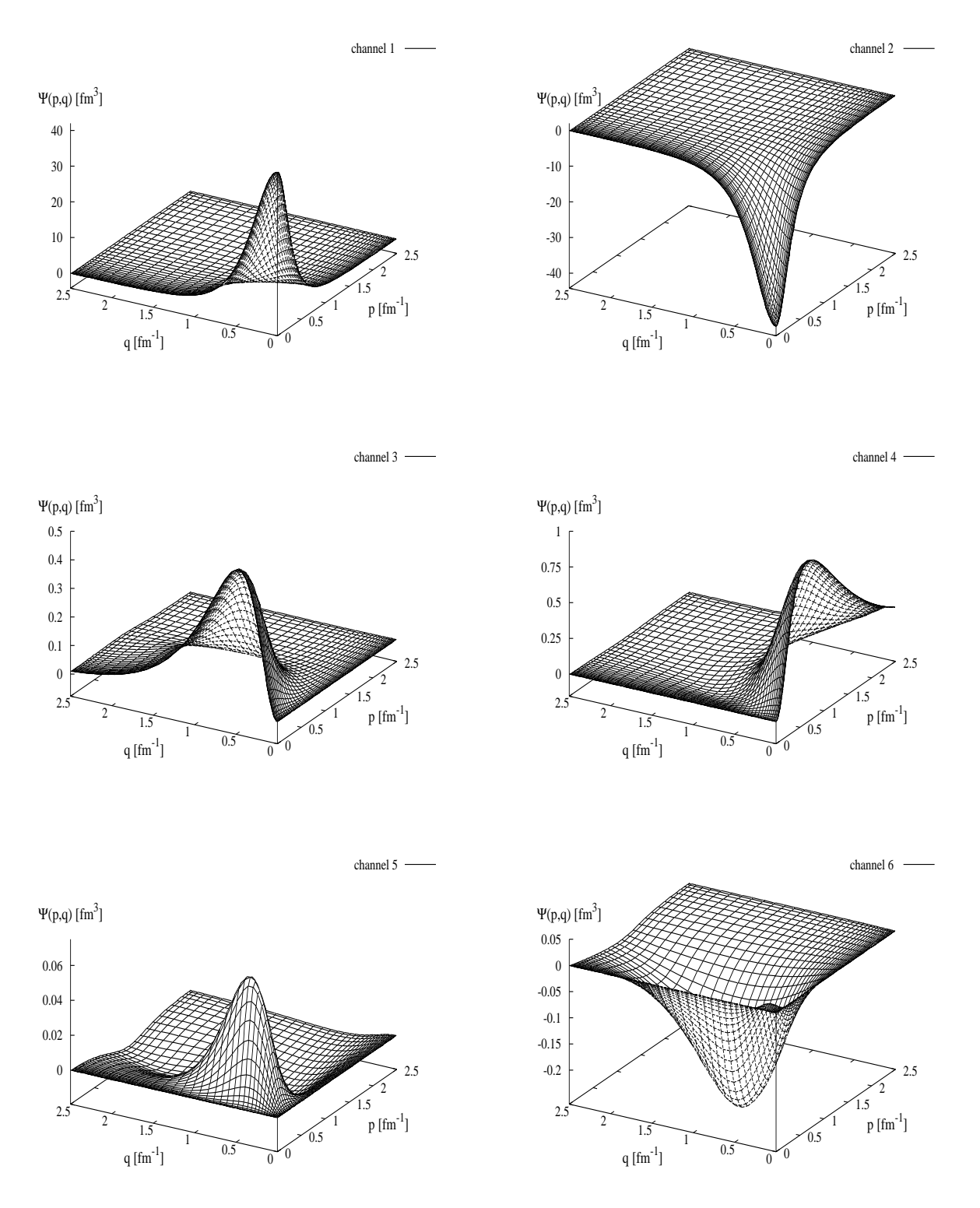
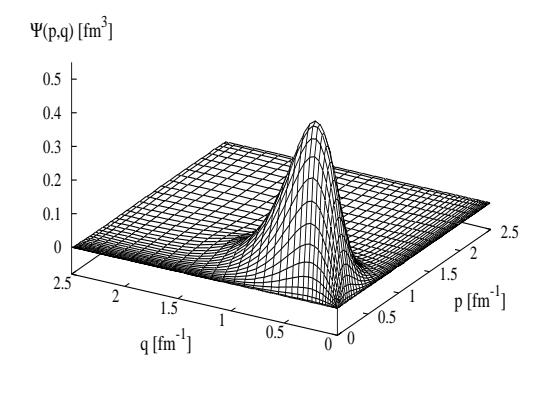
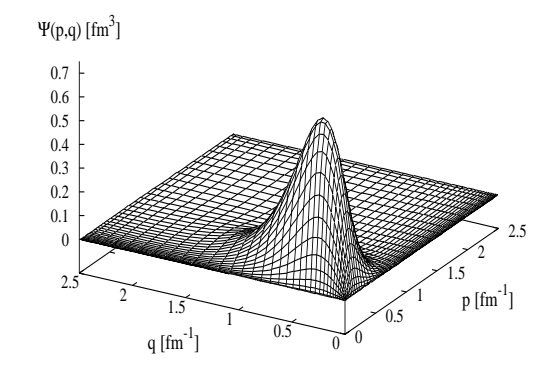
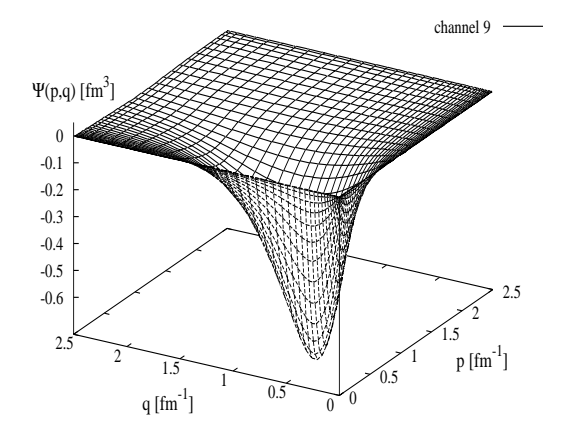


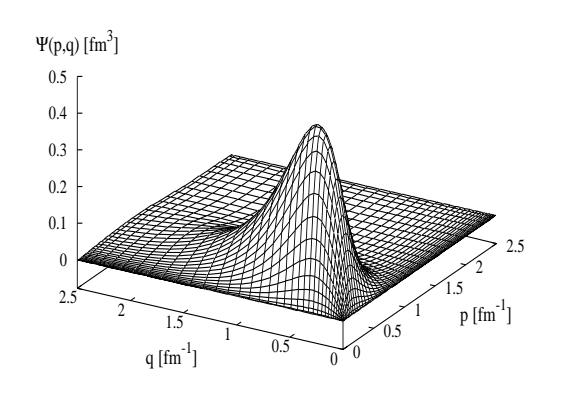
FIG. 1. Graphs of the triton wave function obtained with the Paris (EST) potential. The channels are defined in Table II.

channel 7 —— channel 8 ——

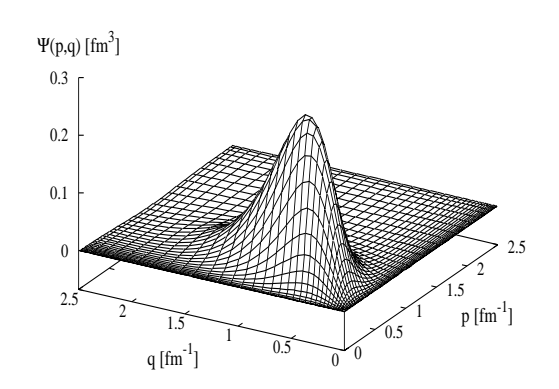








channel 10



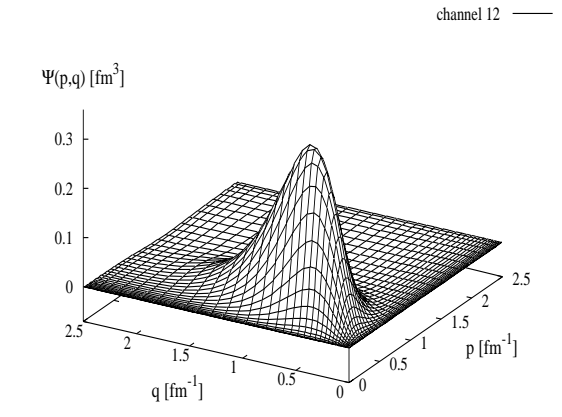


FIG. 2. – continued.

channel 11 -

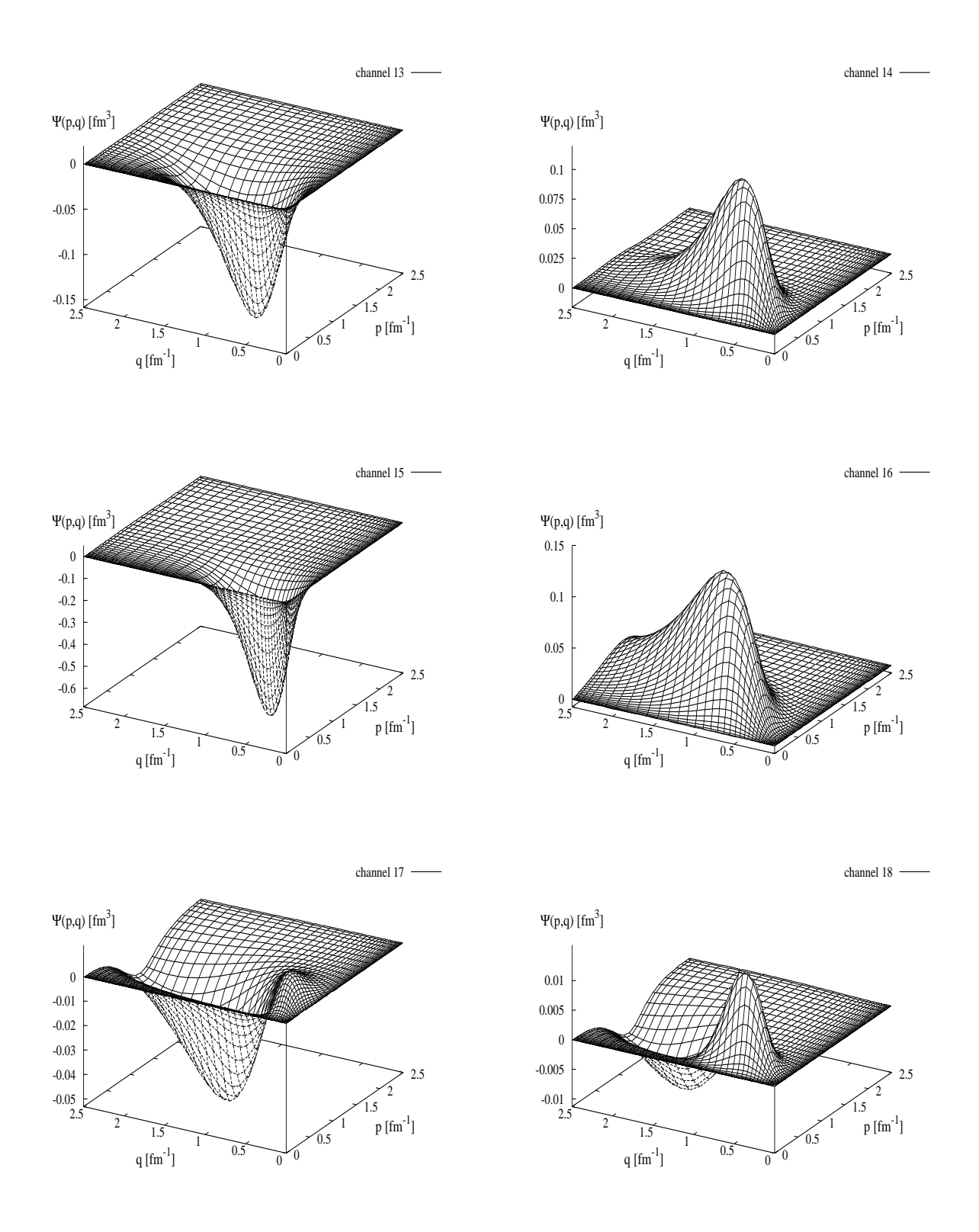


FIG. 3. – continued.

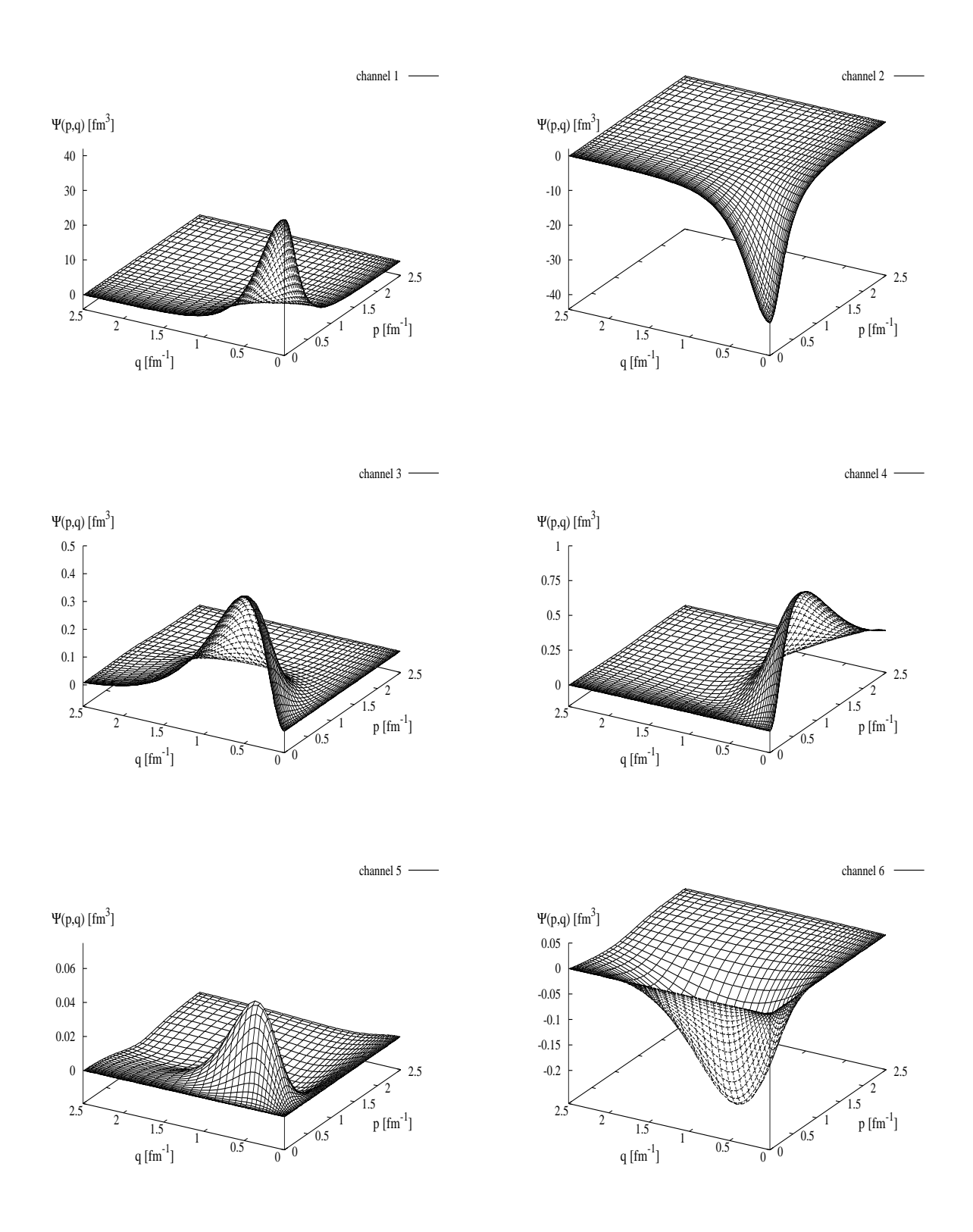


FIG. 4. Same as Fig. 1 but for the Bonn A (EST) potential.



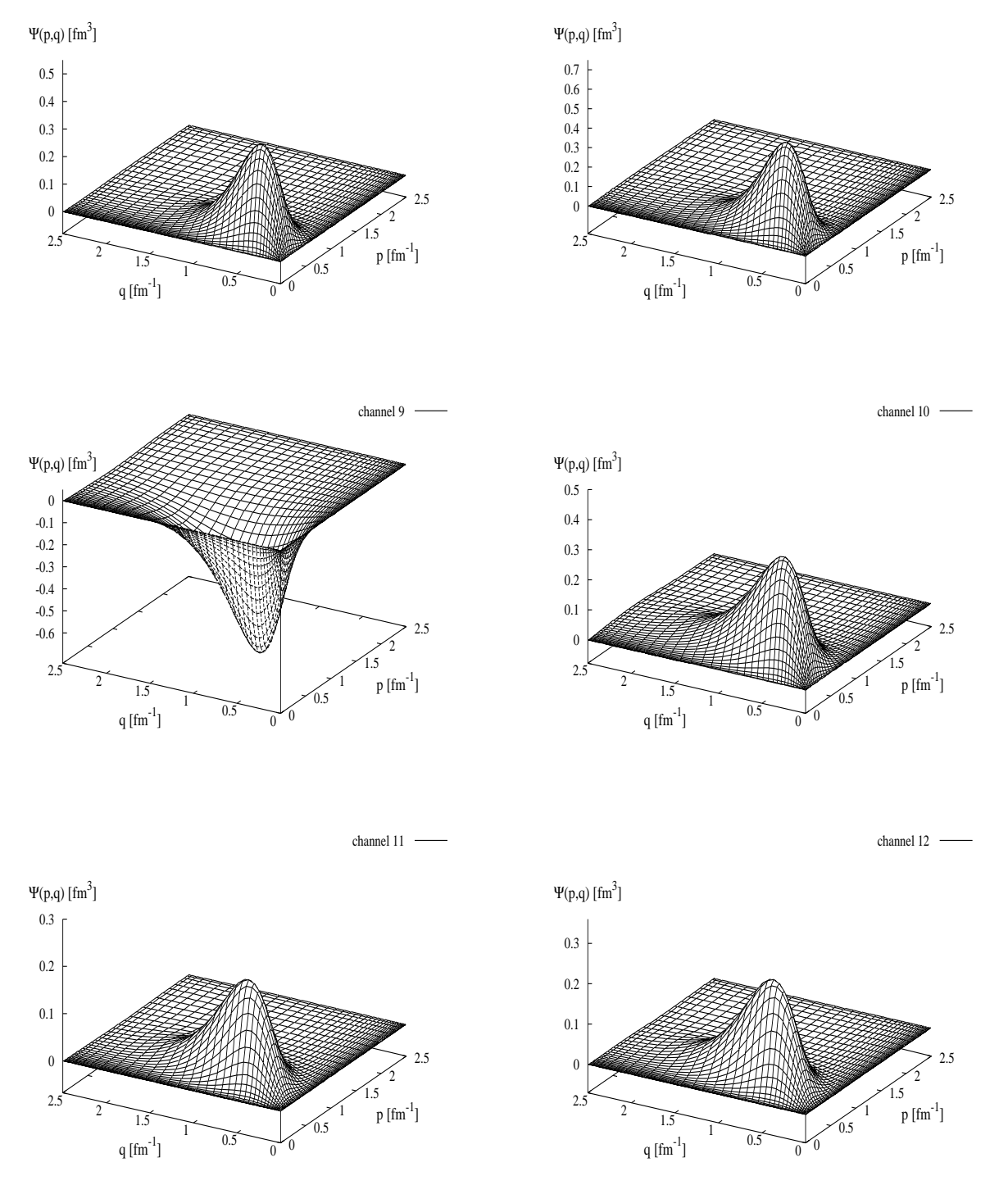


FIG. 5. – continued.

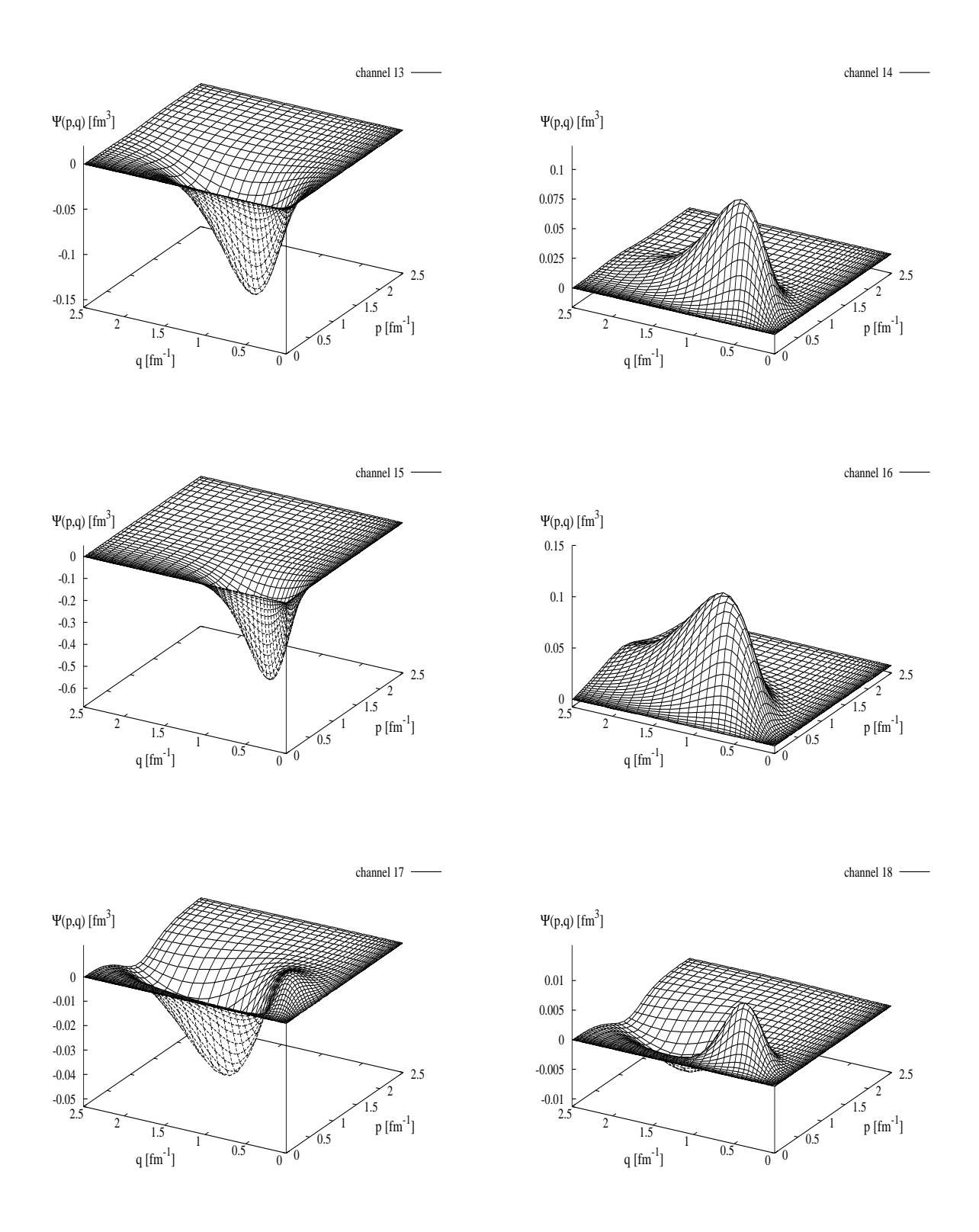


FIG. 6. – continued.